An Experimental Study on the Mass Transfer Process of CO_2 from Liquid CO_2 Drops under Simulated Deep-Sea Conditions

Akihiro Yamasaki (akihiroy@nimc.go.jp)
Keiichi Ogasawara
Ho Teng
National Institute of Materials and Chemical Research
1-1 Higashi, Tsukuba 3058565, JAPAN

Satoko Takano
Minoru Fujii
Yukio Yanagisawa
School of Frontier Science, Institute of Environmental Studies, The University of Tokyo,7-3-1 Hongo, Bunkyo-ku, Tokyo 1138656, JAPAN

Abstract

Mass transfer behavior of CO_2 from liquid CO_2 drops under simulated deep-sea conditions has been studied in a laboratory scale experimental apparatus. Liquid CO_2 was injected into the water of high pressure (p > 50 bar) and low temperature (T < 288 K) conditions through a nozzle. After injection, liquid CO_2 drop of several mm diameter formed in the water phase. The diameter of the drop decreased with time due to the dissolution of CO_2 to the water phase. The interphase mass transfer rate could be expressed in terms of the overall mass transfer coefficient, k_{ov}, as follows,

$$k_{OV} = \left(\frac{C_L}{C_L - C_W} \right) \left| \frac{dr}{dt} \right|$$

where C_L and C_w are the concentrations of CO_2 in the drop, and in the ambient water, respectively. /dr/dt/ is the decreasing rate of the CO_2 drop diameter. The overall mass transfer coefficient depended on the temperature, the pressure, the flow rate of the ambient water, and the existence of CO_2 hydrate film. Formation of the CO_2 hydrate film depended on the injection conditions of liquid CO_2. In some cases, no hydrate formation was noticed during the experiment even the thermodynamic conditions of

hydrate formation (p > 50 bar and T < 283 K) were satisfied. In these cases, the mass transfer coefficient was about one order magnitude higher than the cases with the hydrate film under the same conditions. For the cases with hydrate film, the mass transfer coefficient slightly increased with an increase in the temperature and the ambient flow rate, but decreased with the pressure. The results would provide the basic information for the fate of the liquid CO_2 disposed of in the deep ocean, and consequently the environmental impact caused by the CO_2 disposal process as a counteraction to global warming.

Introduction

Ocean sequestration of CO_2 has been widely recognized as an effective counteraction to global warming [1], [2]. In this scenario, CO_2 emitted by concentrated sources such as thermal power plant and steel industry would be separated and collected from flue gas. The CO_2 thus captured would be disposed of in the ocean. The ocean sequestration scenarios could be categorized into several types in terms of the form of disposed CO_2: dissolution of gaseous CO_2 in the shallow waters (< 500 m), dissolution of liquid CO_2 in the mid waters (500 to 1000 m), deep sea sequestration in the form of liquid CO_2 (> 3000 m), or in the form of solid like dry ice or CO_2 hydrate particle. The choice of the proper scenario may depend on the cost, energy consumption as well as the potential impact to the marine ecosystem both in short and long terms.

To estimate the environmental impact caused by the CO_2 disposed of in the ocean, the mass transfer behavior of CO_2 under the condition of the ocean should be of primary importance. The hydrate formation could make the situation more complicated. For the majority of the disposal scenarios, the disposal depth is deeper than 500 m. Under such conditions of high pressure (> 44.5 bar) and low temperature (< 283 K) [3], CO_2 would form CO_2 hydrate with water, which in turn may significantly affect the mass transfer behavior of CO_2.

The mass transfer behavior of CO_2 under deep-sea conditions has been studied by several authors [4]-[10]. From the laboratory simulation on the behavior of liquid CO_2 in the ocean, the discharged liquid CO_2 would form drops that are covered by a thin film of CO_2 hydrate. The interphase mass transfer of CO_2 may significantly be affected by the hydrate film shown by several authors. However, the previous studies are limited to the conditions for without ambient flow or with ambient flow at low flow rate regions. Considering the real ocean conditions, more systematic study is needed for wide range of the flow rate. Therefore, the target of the present study was to collect experimental information on the behavior of CO_2 drops in a wide range of ambient flow

conditions. In this study, two types of experiments were conducted: mass transfer from suspended liquid CO_2 drops, and mass transfer from CO_2 drops under forced flow conditions. The former experiments correspond to mass transfer from a buoyant CO_2 drops. The experimental results were analyzed, and correlation equations were obtained based on the results.

Experimental

Experimental system

Figure 1 is an experimental apparatus. The main part of the experimental system was a tapered polycarbonate tube, of which the inner diameter was 40 mm at the top and 60 mm at the bottom. The length of the tube was 200 mm. The maximum bearing pressure of the tube was 300 bar. The main part was connected to a water circulation system that was driven by a high-pressure pump, which could generate water flow up to 6.4 L/min. The pressure control of the system was conducted by a piston-type pressure regulator in the range of ± 0.3 bar of the target value. The temperature of the system was controlled with an accuracy of ± 0.3 K through a heat exchanger installed in the circulation system.

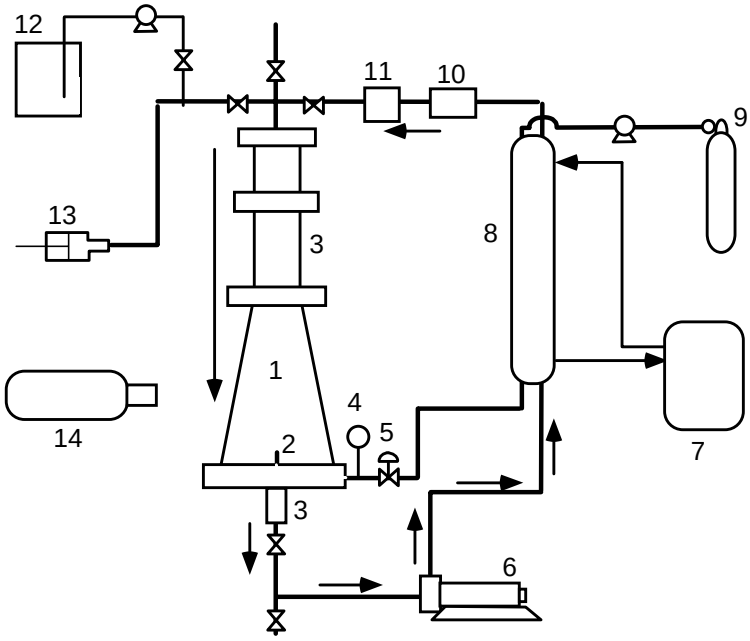

1.Polycarbonate tube; 2.CO_2 injection nozzle; 3.Flow stabilizer; 4.Pressure gauge; 5.Needle valve; 6.high-pressure pump; 7.Thermal bath; 8.Heat exchanger; 9.CO_2 cylinder; 10.Thermometer; 11.Flow rate transducer; 12.Water tank; 13.Piston pump with pressure controller; 14.CCD camera.

Fig. 1 Schematic diagram for the experimental apparatus.

Results and Discussions

Mass transfer of CO_2 from buoyant liquid CO_2 drop-Low Reynolds number region

Method

The mass transfer process of CO_2 from liquid CO_2 drop was conducted as follows. First, the total system was filled with water at an atmospheric pressure. Next, the whole system was pressurized to a certain value, which we call the initial pressure hereafter. The liquid CO_2 was then injected from cylinder to the system through a nozzle at the bottom of the main part of the experimental system. The injection pressure was 65 bar, which was equal to that of CO_2 in the cylinder. The nozzle diameter was 2 mm. Upon injection of liquid CO_2, the system pressure was controlled through the pressure controlling system, and the water circulation was started at a given flow rate. Two types of experiments were conducted: mass transfer from suspended liquid CO_2 drops, and mass transfer from liquid CO_2 drops at constant flow rate. For the former case, the flow rate was controlled so that the buoyancy of the drop was balanced by the drag force by the counter flow. For the latter case, the liquid CO_2 drop was stopped by a metal net at the top of the observation part. The behavior of the drop, that is the shrinking rate, was recorded by a digital CCD camera, and the captured image was analyzed by PC. The formation of CO_2 hydrate film was controlled by the initial pressure before the injection of CO_2. When the initial pressure was higher than 31 bar, the hydrate film was not formed even the pressure and temperature conditions were in the hydrate formation region. On the other hand, the initial pressure was lower than 19 bar, the hydrate film was formed immediately after injection. No clear tendency was observed for the hydrate film formation when the initial water pressure was from 19 to 32 bar.

Results and Discussions

Figure 2 shows a typical time course of drop diameter change of CO_2 drop. The drop was covered with hydrate film; the temperature was 278 K, and the pressure was 55 bar. The drop diameter decreased with time due to dissolution of CO_2 in water. Similar results were obtained for other conditions. Such shrinking processes could be expressed by the following material balance equation (1).

$$\left| \frac{d}{dt}\left(\frac{4}{3}\pi r^3 C_0 \right) \right| = 4\pi r^2 k_{ov}(C_0 - C_W) \qquad (1)$$

where r is the droplet radius, k_{ov} is the overall mass transfer coefficient; C_0, C_s, and C_w are the concentration CO_2 in the drop, at the surface of the drop, and at the bulk water, respectively. Since $C_0 \gg C_w$, Eq. (1) can be rearranged to

$$|dr/dt| \approx k_{ov} \quad (2)$$

Equation (2) indicates that the overall mass transfer coefficient approximately equals to the shrinking rate of the CO_2 drop. The drop diameter linearly decreased with the suspension time, which indicating a constant mass transfer coefficient during the dissolution process. Figure 3 shows effect of temperature on the overall mass transfer coefficients. The overall mass transfer coefficient increased with an increase in the temperature for both cases with and without hydrate film. For a given temperature, overall mass transfer coefficient with hydrate film was one order of magnitude smaller than that without hydrate film. On the other hand, for a given temperature, the overall mass transfer coefficient decreased with an increase in the pressure as shown in Figure 5.

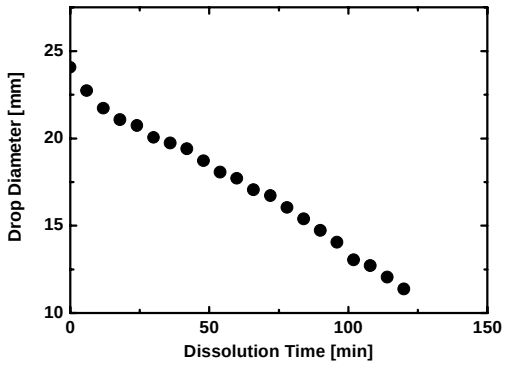

Figure 3 Time course of drop diameter covered with hydrate film, Temperature = 278 K, Pressure = 55 bar.

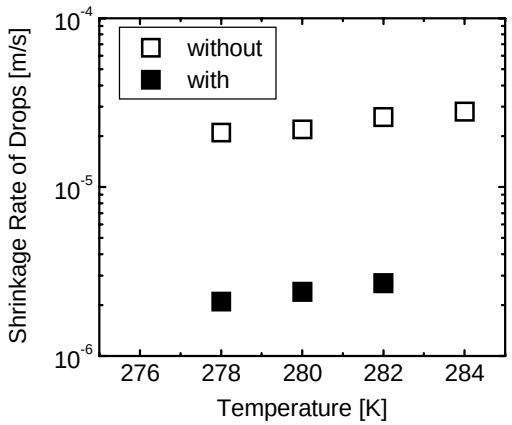

Fig. 4 Effect of temperature on the drop shrinking rate with and without hydrate film (pressure=55 bar).

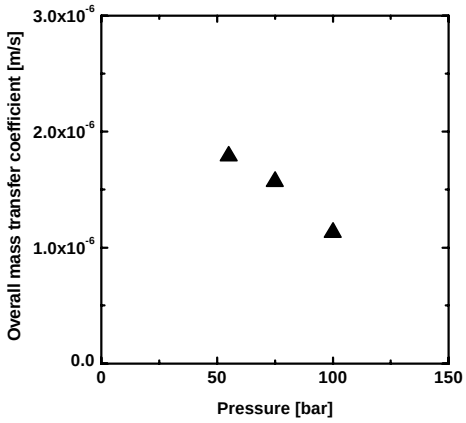

Fig. 5 Effect of pressure on the drop shrinking rate with hydrate film (Temperature 278 K).

Mass transfer of CO_2 from liquid CO_2 drop under flow conditions- High Reynolds number region

Methods

In this case, the ambient flow rate was kept constant during the dissolution process of drops. With the decrease in the drop diameter, the position of the drop drift. To keep the drops in the observation section, a metal mesh was at the top of the polycarbonate tube. The same procedure was applied for preparing with/without hydrate film conditions.

Results and Discussions

Figure 6 shows the results for the mass transfer coefficient as a function of Reynolds number (based on the drop size). The Reynolds number in this study was defined based on the drop diameter. Since the drop diameter changes constantly, the results shown in Figure 6 is average values for 3 to 5 min interval. The mass transfer coefficient increased with an increase in Reynolds number. The dependence of the mass transfer coefficient can be correlated with the following equations for the case of liquid drops without hydrate formation.

$$k_L = 1.97\times10^{-7} + 7.48\times10^{-7}\ \mathrm{Re}^{0.290} \qquad (3)$$

where mass transfer coefficient in the boundary layer of water phase k_L was obtained by,

$$k_{OV} = \frac{C^*}{C_0} k_L \qquad (4)$$

assuming the mass transfer resistance for the dissolution process is concentrated in the boundary layer. C^* is the equilibrium concentration of CO_2 in the water phase.

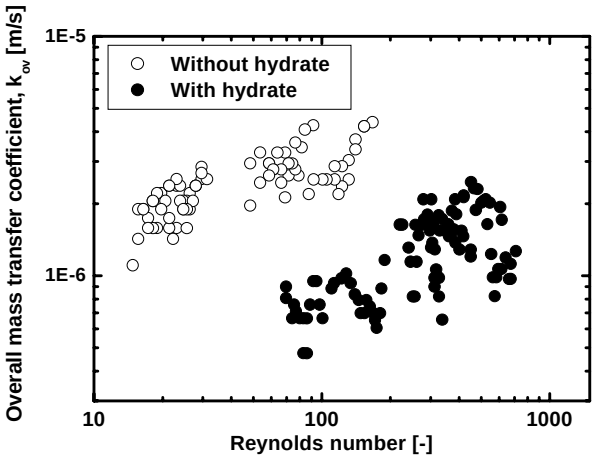

Figure 6 Overall mass transfer coefficient as a function of Reynolds number.

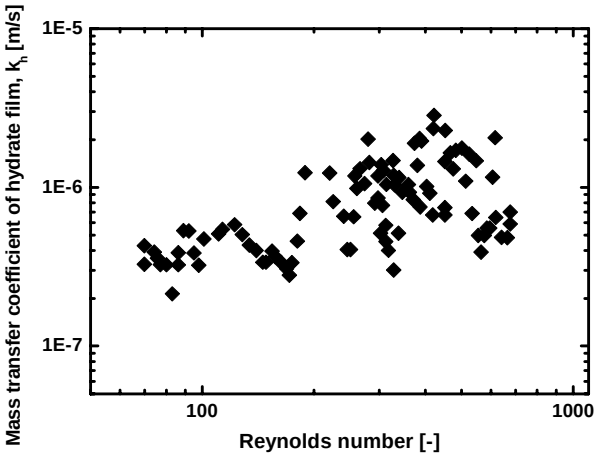

Figure 7 Mass transfer coefficient for the hydrate layer as a function of Reynolds number.

For the mass transfer process with hydrate film, a series resistance model is proposed; the mass transfer resistance for CO_2 from the drops is assumed to be composed of; (1) mass transfer in hydrate film, k_h, (2) formation and dissociation of hydrate film at the interface of hydrate film and water, (3) mass transfer in the diffusion boundary layer in the water phase, k_L. The mass transfer flux is given by,

$$J = k_h(C_{h1} - C_{h2}) = k_L(sC_{h2} - C_W) = k_{OV}(C_0 - C_w) \tag{5}$$

$$\frac{1}{k_{OV}} = \frac{C_0}{C_{h1}}\left(\frac{1}{k_h} + \frac{C_{h2}}{C_i}\frac{1}{k_L}\right) \tag{6}$$

It is assumed that hydrate formation and dissociation equilibria are assumed both at the interfaces of hydrate film/ water, and the liquid CO_2/ the hydrate film. The equilibrium concentration of CO_2 at the interface of CO_2 and hydrate would be the value C_{h1} corresponding to the maximum occupancy of CO_2 molecules in the hydrate lattice (CO_2 + 5.75 H_2O), because enough amount of CO_2 should be always supplied from the drop phase (C_{h1} = 7.69 kmol/m^3) [11]. The equilibrium concentration of CO_2 at the interface of hydrate and water phase depends on the phase. The CO_2 concentration at the interface of the hydrate and water phase should be the one (C_{h2}=4.80 kmol/m^3) corresponding to the critical CO_2 occupancy which can stabilize the hydrate structure, x = 0.099 [11]. Although the CO_2 at the interface of water and hydrate is supersaturated, we assume a simple relationship between C_{h2}=C_i, where C_i is the CO_2 concentration at the interface in water phase.

To estimate the contributions from each mass transfer resistance, it was assumed that the mass transfer coefficient in the water phase equals to the one without hydrate film for the same Reynolds number condition. Thus, k_L, and k_h could be obtained as a function of Reynolds number. Figure 7 shows the results for the Reynolds number dependency of k_h. The mass transfer coefficient through the hydrate film increased with an increase in the Reynolds number. Since the mass transfer coefficient through the hydrate film is given by,

$$k_h = \frac{D_h}{\delta} \tag{7}$$

where D_h is the diffusion coefficient of CO_2 in the hydrate film, δ is the thickness of the hydrate film. The increase in the mass transfer coefficient with an increasing Reynolds number suggests that the hydrate film thickness decreases with the flow rate. The absolute value of the mass transfer coefficient is in the range of 10^{-6} m/s.

Mass transfer of CO_2 in seawater

Figure 8 shows the overall mass transfer coefficients as a function of Reynolds number. No large differences were observed for pure water cases.

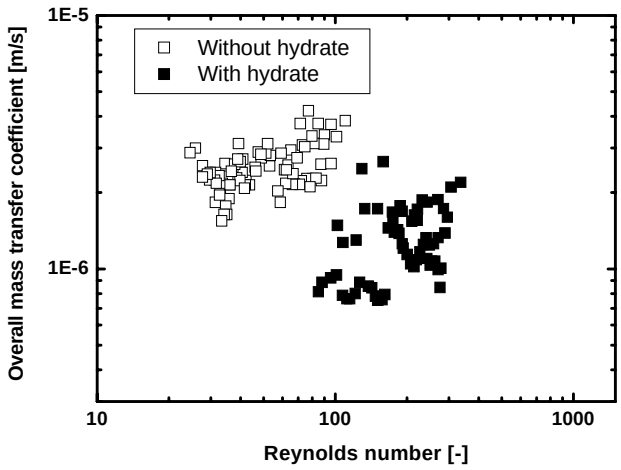

Figure 8 Overall mass transfer coefficient as a function of Reynolds number in artificial seawater.

Conclusions

Experimental studies on the mass transfer of CO_2 from liquid CO_2 drops were conducted in simulated deep-sea conditions. The mass transfer rate was obtained as mass transfer coefficients as a function of Reynolds number. It was found that the hydrate film on at the surface of liquid CO_2 drops significantly reduced the mass transfer rate.

References

(1) Halmann, M. M.; Steinberg, M., "*Greenhouse Gas Carbon Dioxide Mitigation*", Lewis, Boca Raton, FL (1999).

(2) Handa N. ; Ohsumi, T., "*Direct Ocean Disposal of Carbon Dioxide*", Terra Scientific Publishing Company, Tokyo (1995).

(3) Song, K. Y.; Kobayashi, R., SPE Formation Evaluation, Societies of Petroleum Engineers, 500-508 (1987).

(4) Aya, I.; Yamane, K.; Yamada, N., *Energy Convs. Mgmnt.*, **1995**, *36*, 485-488.

(5) Shindo, Y.; Fujioka, Y.; Takenouchi, K.; Komiyama, H. *Int. J. Chem. Kinet.*, **1995**, *27*, 569-575.

(6) Nishikawa, N.; Ishibashi, M.; Ohta, H.; Akutsu, N.; Tajika, M.; Sugitani, T.; Hiraoka, R.; Kimuro, H.; Shiota, T. *Energy Convs. Mgmnt.*, **1995**, *36*, 489-492.

(7) Hirai, S.; Okazaki, K.; Araki, N.; Yazawa, H.; Ito, H.; Hijikata K. *Energy Convs. Mgmnt.*, **1996,** *37*, 1073-1078.
(8) Hirai, S.; Okazaki, K.; Tabe, Y.; Hijikata, K.; Mori, Y., Energy, **1997**, *22*, 285-293.
(9) Warzinski, R. P.; Cugini, A. V.; Holder, G. D. *Coal Science*, (J. A. Pajares and J. M. D. Tascon eds.), **1995**, 1931-1935.
(10) Holder, G. D.; Cugini, A. V.; Warzinski, R. P. *Environ. Sci. Technol.*, **1995**, 29, 276-278.
(11) Teng, H.; Yamasaki, A.; Shindo, Y. *Chem. Eng. Sci.*, **1996**, *51*, 4979-4986.